CONDENSED-MATTER
SPECTROSCOPY

Raman Scattering in Lead Selenide Films at a Low Excitation Level

M. O. Kuzivanov[a], S. P. Zimin[b], A. V. Fedorov[a], and A. V. Baranov[a]
[a] ITMO University, St. Petersburg, 197101 Russia
[b] Demidov Yaroslavl State University, Yaroslavl, 150000 Russia
e-mail: mkuzivanov@mail.ru
Received June 19, 2015

Abstract—Raman scattering spectra of epitaxial lead selenide films were measured at low (0.06 mW/μm^2) excitation power densities to ensure the absence of photo- and thermal modifications of the film material. It is shown that observed transitions correspond to overtones or combinational tones of PbSe phonon modes implying a high quality of crystalline structure of the material for which the first order Raman effect is prohibited. An increase in incident excitation density leads to the appearance of transitions related to lead oxides, which masks characteristic spectral features of lead selenide.

INTRODUCTION

Raman scattering (RS) spectroscopy allows one to determine the phonon modes in studied samples and to obtain information on the chemical composition of the studied material and its crystalline structure, as well as on the presence of extraneous phases and areas with a local order (disorder) of the crystalline lattice [1]. Raman spectroscopy is widely used for studies and characterization of nanomaterials without destruction or modification of their structures [2]. It is known that similar knowledge can be obtained using the transmission electron microscopy and X-ray diffraction methods. However, in comparison with those methods that require vacuum equipment, time demanding preparation to measurements and often cause destruction of the studied objects, Raman spectroscopy is a more convenient method for fast and nondestructive analysis [3].

Studies of lead chalcogenide PbX (X = Te, Se, S) compounds are of significant interest related to applications of these narrow-band materials in optoelectronic including, in particular, injection lasers and light detectors for the mid-IR region [4, 5], thermoelectric and solar energy converters [6]. Variation of the mole fraction x in ternary solid solutions such as $Pb_{1-x}Sn_xSe$ and $Pb_{1-x}Eu_xSe$, allows a controlled modification of their electro-physical and optical characteristics. These compounds are widely used to make Bragg mirrors [7] and microresonators for the vertical cavity surface emitting lasers [8]. However, application of Raman spectroscopy for studies of binary lead chalcogenide compounds and their ternary solid solutions is hampered by a number of obsta-

cles related to the restriction of the first order RS by symmetry under normal conditions, as well as thermo- and photo-instability of these materials [1, 9].

Analysis of experimental results in [10–14] shows that rather intense bands in observed Raman spectra in most cases are assigned to transverse (TO) and longitudinal (LO) PbSe phonons (Table 1) although these transitions are symmetry forbidden. Assignment of these transitions in Raman spectra is important because their positions are used as a ground for conclusions on modification of the crystalline structure after various manipulations with the PbSe crystal (doping, reducing the size to a few nanometers, etc.) [10–13].

As it has been shown in our earlier work [1] for the case of PbTe films, measurements of correct Raman spectra of strongly absorbing and photosensitive lead chalcogenides require as low power density of the exciting laser radiation as possible. The aim of the present work was a comprehensive study of Raman spectra of epitaxial lead selenide films under conditions minimizing the power density of incident laser radiation and comparison with the results obtained at

Table 1. Assignment of some transitions in Raman spectra to PbSe phonon modes [10–14]

	[10]	[11]	[12]	[13]	[14]
TO, cm^{-1}	–	47	–	–	47.6
LO, cm^{-1}	135	139.6	140	128	135
2LO, cm^{-1}	238	270	281	238	270

a higher power density, as well as with the literature data.

EXPERIMENTAL

The studies were performed on epitaxial PbSe films grown on Si(111) substrates using a molecular beam epitaxy (MBE) technique with 2- to 4-nm-thick CaF_2 buffer layers as proposed in [4, 8]. PbSe films with a thickness of 2–4 μm were grown at a substrate temperature of 350–400°C. X-ray diffraction analysis (Fig. 1) showed a high structural perfection of single-phase (111)-oriented PbSe films.

Additional comparative measurements were performed on $Pb_{1-x}Eu_xSe$ films with europium molar fractions x in the 0.03–0.16 region and the layers of $Pb_{1-x}Sn_xSe$ with x in the 0.03–0.06 region, obtained using a similar MBE technique. All the studied films had a smooth mirror surface with a characteristic nano profile in the form of a system of triangular nanoterraces and triangular holes corresponding to the outputs of penetrating dislocations. A detailed description of the structural characteristics of the studied films is given in [15].

Raman spectra were recorded in the backscattering geometry at room temperature using a micro-RS InVia spectrometer (Renishaw, United Kingdom). The source of exciting radiation was an Ar^{+2} laser, $\lambda = 514.5$ nm. A peculiar feature of spectra recording was application of a special Renishaw Streamline™ Plus system [1] to minimize the power density of the exciting radiation with no loss in the signal intensity. With use of this system, the exciting radiation with a power of 6 mW is focused onto the sample not in the usual round spot with a diameter of ~2 μm, but in a strip of ~2 × 50 μm². It allowed us to decrease the laser power density on the sample surface by a factor of 50 without any loss in Raman signal intensity because Streamline™ uses a whole 2D system of CCD matrix pixels for recording Raman signal from the whole irradiated area of the sample [16]. It is an important factor in studies of such photo-oxidizing material as PbSe for which recording the weak second-order Raman signals requires a rather intense exciting radiation. In addition, for comparison, we use a standard measuring method in which the exciting radiation with a power of 12 mW is focused into a spot 2 μm in diameter. It should be noted that the rather large film thickness allows one to not take into account the substrate contribution to the Raman signal, because the PbSe absorption coefficient at 515.5 nm is ~5 × 10⁵ cm⁻¹ [17]. Consequently, the penetration depth of the laser radiation into the sample is only ~20 nm.

RESULTS AND DISCUSSION

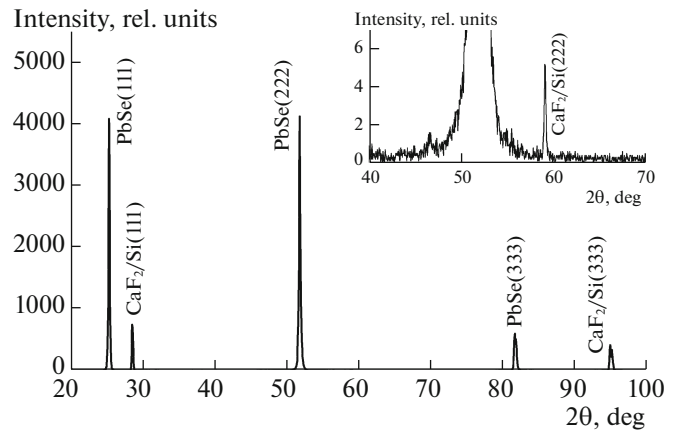A typical Raman spectrum of RbSe films on the $CaF_2/Si(111)$ substrate obtained under conditions

**Fig. 1.** Typical diffraction spectrum of PbSe/CaF_2/Si(111) film measured with the use of a Cu source.

minimizing the power density of exciting radiation with use of the Streamline™ system is shown in Fig. 2a. To confirm the sample homogeneity, the spectra were recorded for three different sample areas and then averaged. An important feature of the recorded spectrum is the presence of an extensive set of Raman transitions in the 50–175 cm⁻¹ region. This transition set, which has not been observed in early studies, is well reproduced in a set of five consecutive measurements. The Stocks shift for the most intense bands is 59, 73, 82, 91, 106, 120, 130, and 138 cm⁻¹. There is also a rich spectral structure in the 200–350 cm⁻¹ region consisting of several overlapping bands of a moderate intensity which most likely correspond to higher-order Raman transitions.

The spectra were analyzed using dispersion curves and frequencies of PbSe phonon modes in different critical points of Brillouin zone calculated in [6]. Corresponding dispersion curves for transverse and longitudinal acoustic modes (TA and LA) and optical (TO and LO) phonons are given in Fig. 2b. Table 2 shows calculated frequencies of phonon modes [6] for a set of critical points of the Brillouin zone which are in a good agreement with the results of other studies [18–21].

Comparison of transition frequencies in the Raman spectrum of the PbSe layer shown in Fig. 2a, with calculated values of phonon frequencies in Table 2 allows one to establish a correspondence between the overtone and combinational phonon

Table 2. Frequencies of phonon modes (cm⁻¹) for some critical points of PbSe Brillouin zone [6]

	LA	TA	LO	TO
Γ	–	–	128	34
X	45	33	84	70
L	97	51	139	120
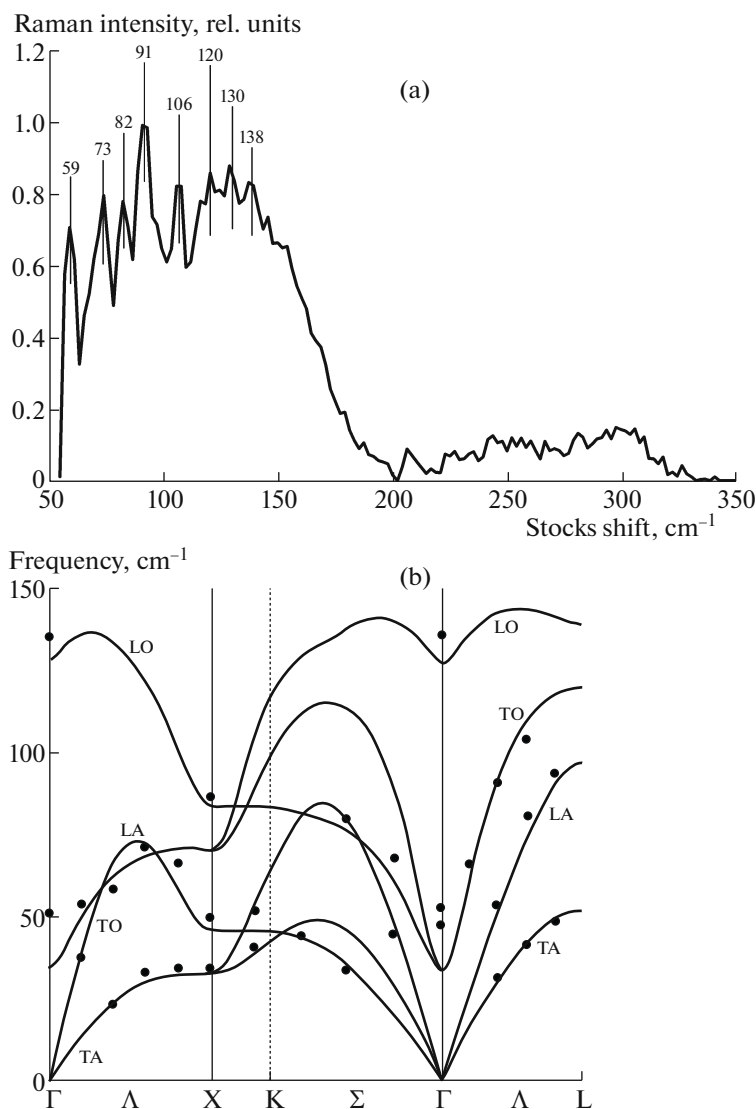
Fig. 2. (a) Typical Raman spectrum of an epitaxial PbSe film on CaF_2/Si(111) substrate. The wavenumbers of main transitions are given. (b) Calculated dispersion curves for the PbSe crystal [6].

tones at different critical points of the Brillouin zone. The assignment is given in Table 3.

Analysis of the obtained results allows one to exclude the effect of surface photo-oxidation because spectra show no characteristic intense transitions belonging to oxides of lead [22, 23] and selenium [24, 25] and, thus, the experimental Raman spectrum may be considered as solely due to PbSe phonons with no contributions from other phases. All observed transitions in the Raman spectrum may be unambiguously assigned to overtones or combinational tones of phonon modes. This fact implies that the first order Raman effect is indeed forbidden in the studied PbSe films.

Table 3. Assignment of transitions in Raman spectra of epitaxial RbSe films to overtones and combinational tones of phonons at different critical points of the Brillouin zone

59 cm^{-1}	73 cm^{-1}	82 cm^{-1}	91 cm^{-1}	106 cm^{-1}	120 cm^{-1}	130 cm^{-1}	138 cm^{-1}
2TA(X)	LA(X)+TA(X) and/or 2TO(Γ)	LA(X)+TA(X)	2LA(X)	2TA(L) and/or TA(X)+TO(X)	LA(X)+TO(X) and/or TA(X)+LO(X)	LA(X)+LO(X)	2TO(X)
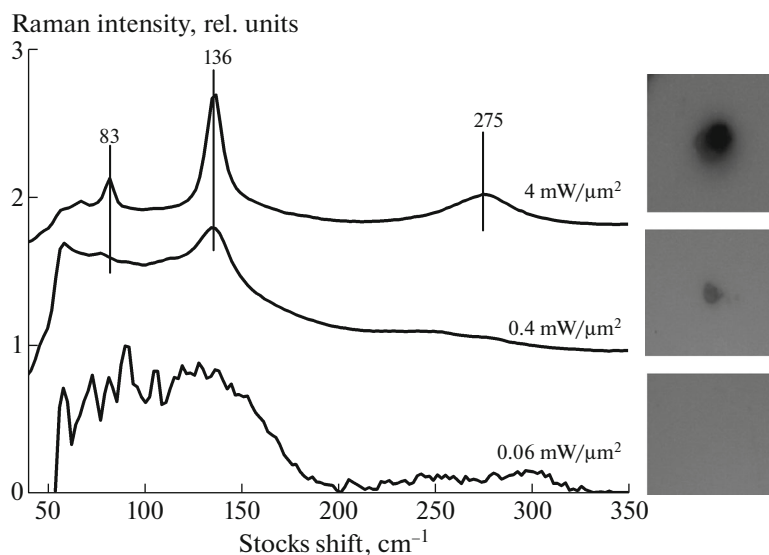
Fig. 3. Raman spectra of PbSe films at power densities of exciting radiation of 0.06, 0.4, 4 mW/μm². Raman transition frequencies are given. Insert shows corresponding microphotos (10 × 10 μm) of sample surfaces after exposure to exciting radiation.

To explain the differences in published Raman spectra of PbSe we studied changes in the measured spectra on the power density of exciting laser radiation in the 0.06−4 mW/μm² region. The results are given in Fig. 3. As is seen from these spectra, the increase in the power density results in appearance of transitions at 83, 136, and 275 cm⁻¹, which are typical for lead oxides of different crystalline modifications after the laser treatment of the sample surface [22]. Thus, we can assume that PbSe under a strong laser exposure loses selenium and interacts with oxygen forming oxide phases PbO_x, which eventually transforms into the described in [22] modification with three characteristic transitions in the Raman spectrum. Concomitant modification of the surface of PbSe films is clearly seen in the objective lens focal region with use of a built-in optical microscope of our micro Raman spectrometer, as is shown in the right part of Fig. 3. The transition frequencies in the spectra recorded in this way practically coincide with transitions observed earlier in [10−14] at power densities of exciting radiation above ~1.3 mW/μm² [12], which were erroneously assigned to PbSe. The slight discrepancies in the published spectra may be due to the formation of different modifications of lead oxides at different powers of incident radiation [22].

Studies of ternary solid solution $Pb_{1-x}Sn_xSe$ ($x \leqslant$ 0.06) and $Pb_{1-x}Eu_xSe$ ($x \leqslant$ 0.16) showed that within the experimental uncertainty region their Raman spectra reproduce the spectrum of the binary PbSe compound (Fig. 2a). One may conclude that doping with small amount of Sn (up to 6%) or Eu (up to 16%) has no effect on the crystalline lattice and the energy spectrum of PbSe phonons and cannot break up the symmetry restriction on the first-order Raman effect in PbSe.

CONCLUSIONS

Raman spectra of PbSe films were measured for the first time under conditions minimizing the exciting radiation power to ensure the absence of photo- and thermo-induced sample modifications. The spectra display an extensive set of transitions in the 50−175 cm⁻¹ region, all of which can be assigned to overtones or combinational tones of phonon modes of this material. The absence in the spectra of the first-order Raman transition implies high quality of the crystalline structure of the studied samples for which the first-order effect is forbidden by symmetry. It is shown that intense transitions that were observed in previous studies at 136 and 275 cm⁻¹, which were assigned to the LO and 2LO phonons of PbSe, are actually due to active photo-oxidation processes under the laser radiation exposure and belong to lead oxides.

ACKNOWLEDGMENTS

REFERENCES

1. S. P. Zimin, E. S. Gorlachev, A. V. Baranov, S. A. Cherevkov, E. Abramof, and P. H. O. Rappl, Opt. Spectrosc. **117**, 748 (2014).

2. A. V. Baranov, K. V. Bogdanov, E. V. Ushakova, S. A. Cherevkov, A. V. Fedorov, and S. Tscharntke, Opt. Spectrosc. **109**, 268 (2010).

3. S. A. Cherevkov and A. V. Baranov, Nauch.-Tekh. Vestn. SPbGU ITMO **51**, 286 (2008).

4. H. Zogg, A. Fach, J. John, J. Masek, P. Mueller, C. Paglino, and S. Blunier, Opt. Eng. **34**, 1964 (1995).

5. M. Tacke, Philos. Trans. A **359**, 547 (2001).

6. O. Kilian, G. Allan, and L. Wirtz, Phys. Rev. B **80**, 245208 (2009).

7. T. Schwarzl, G. Springholz, M. Böberl, E. Kaufmann, J. Roither, W. Heiss, J. Furst, and H. Pascher, Appl. Phys. Lett. **86**, 031102 (2005).

8. H. Zogg, K. Kellermann, K. Alchalabi, and D. Zimin, Infrared Phys. Technol. **46**, 155 (2004).

9. S. P. Zimin, E. S. Gorlachev, N. V. Gladysheva, V. V. Naumov, V. F. Gremenok, and H. G. Seidi, Opt. Spectrosc. **115**, 679 (2013).

10. V. Arivazhagan, M. Manonmani Parvathi, and S. Rajesh, J. Alloys Compd. **577**, 431 (2013).

11. C. Gayner and K. K. Kar, J. Appl. Phys. **117**, 103906 (2015).

12. J. Habinshuti, O. Kilian, O. Cristini-Robbe, A. Sashchiuk, A. Addad, S. Turrell, E. Lifshitz, B. Grandidier, and L. Wirtz, Phys. Rev. B **88**, 115313 (2013).

13. M. Manonmani Parvathi, V. Arivazhagan, and S. Rajesh, Appl. Phys. A **116**, 1773 (2014).

14. A.-L. Yang, H.-Z. Wu, Z.-F. Li, D.-J. Qiu, Y. Chang, J.-F. Li, P. J. McCann, and X. M. Fang, Chin. Phys. Lett. **17**, 606 (2000).

15. S. P. Zimin, E. A. Bogoyavlenskaya, E. S. Gorlachev, V. V. Naumov, D. S. Zimin, H. Zogg, and M. Arnold, Semicond. Sci. Technol. **22**, 1317 (2007).

16. http://www.renishaw.com/en/streamline-generate-chemical-images-rapidly-9449

17. N. Suzuki, K. Sawai, and S. Adachi, J. Appl. Phys. **77**, 1249 (1995).

18. A. H. Romero, M. Cardona, R. K. Kremer, R. Lauck, G. Siegle, J. Serrano, and X. C. Gonze, Phys. Rev. B **78**, 224302 (2008).

19. Z. Tian, J. Garg, K. Esfarjani, T. Shiga, J. Shiomi, and G. Chen, Phys. Rev. B **85**, 184303 (2012).

20. K. S. Upadhyaya, M. Yadav, and G. K. Upadhyaya, Phys. Status Solidi B **229**, 1129 (2002).

21. Y. Zhang, X. Ke, C. Chen, J. Yang, and P. R. C. Kent, Phys. Rev. B **80**, 024304 (2009).

22. L. Burgio, R. J. H. Clark, and S. Firth, Analyst **126**, 222 (2001).

23. M. J. Bierman, Y. K. A. Lau, and S. Jin, Nano Lett. **7**, 2907 (2007).

24. O. A. Balitskii, V. P. Savchyn, and V. O. Yukhymchuk, Semicond. Sci. Technol. **17**, L1 (2002).

25. A. Grzechnik, L. Farina, R. Lauck, K. Syassen, I. Loa, and P. Bouvier, J. Solid State Chem. **168**, 184 (2002).

Translated by V. Alekseev